The influence of peptide structure on fragmentation pathways

Bari, Sadia

Chapter 3

Experiment

The main task of this PhD project was to build a new experimental setup which facilitates studies on keV ion–induced dynamics of free complex biomolecular systems. Electrospray ionization was selected to bring the molecules into vacuum. This technique overcomes the limitation to relatively small target molecules which are stable with respect to thermal decomposition. Dealing with ionic biomolecular systems also allows to employ radio–frequency ion guiding, mass selection and trapping. The accumulation of mass–selected biomolecular ions in a trap was chosen as the most straightforward way of reaching a target density that is high enough for ion collision studies or photodissociation experiments. This chapter will give a complete technical description of the apparatus named Paultje, that was designed, assembled and put into operation in the course of this thesis.

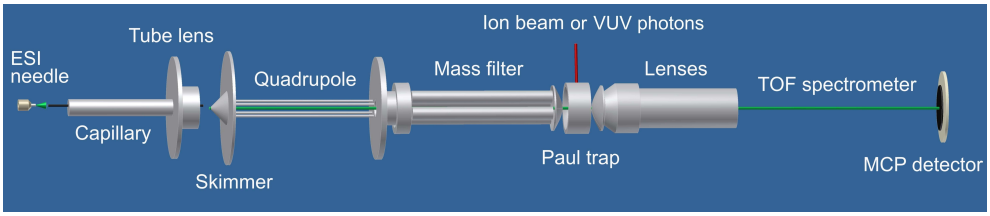

Figure 3.1: *Schematic lay–out of the new experimental setup "Paultje".*

3.1 CHEOPS setup

During the construction phase of the new apparatus experiments with an effusive target of sublimated amino acids (see chapter 4 and 5) were performed with the already existing setup CHEOPS. A short description as well as a sketch of this experimental setup can be found in the experimental part of chapter 4. A more detailed treatise of the setup is given in the PhD theses of the former group members, Omar Hadjar [1] and Fresia Alvarado [2].

3.2 Paultje setup

The Paultje setup is depicted in fig. 3.1 and a photograph is shown in fig. 3.2. Electrosprayed biomolecular ions are focused by a tube lens through a skimmer, guided by an RF–only quadrupole, mass filtered by an RF and DC quadrupole and trapped in a 3D quadrupole ion trap (Paul trap) to get sufficient target density. The trapped target molecules are then exposed to keV ions or VUV photons and the collision products are extracted into a time–of–flight spectrometer and detected by a multi–channel–plate detector. The different stages of the setup and the applied techniques are described in the following.

3.3 Electrospray ionization

Electrospray ionization (ESI) is a gentle technique to introduce large biomolecular ions from solution into the gas phase. J. B. Fenn received the Nobel Prize in Chemistry 2002 for the establishment of ESI for identification and structure analysis of biological macromolecules [3].

In ESI a solution of the analyte is pumped through a metal capillary needle which is held at high potential (in this thesis typically voltages of $\sim +3.6$ kV were used) with respect to the vacuum chamber. The high electric field between the needle and a heated capillary serving as a counter electrode, penetrates the solution and separates the charges in it. The accumulation of the same charge (in our case positive) at the needle tip leads to Coulomb repulsion that gives rise to the formation of a Taylor cone. When the electrostatic repulsion exceeds the surface tension of the solution, small charged droplets are emitted from the Taylor cone (see fig. 3.3). The size of the initial droplets is typically of the order of 0.5 up to several tens of μm depending on parameters such as needle voltage, flow rate and surface tension of the

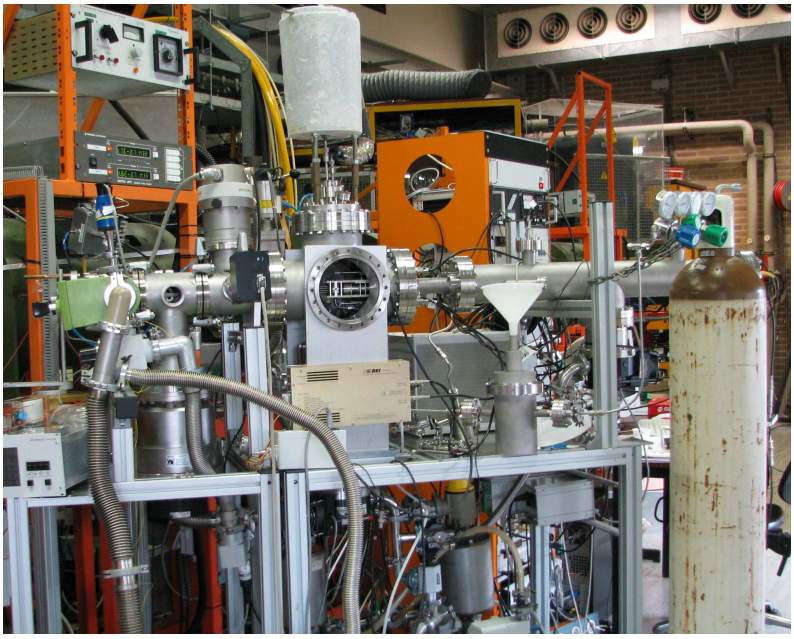

Figure 3.2: *Photograph of the setup.*

solution [4, 5]. During their flight at atmospheric pressure the droplet diameter decreases due to solvent evaporation and the charge density at the droplet surface increases. When the surface tension cannot compensate the Coulomb repulsion of the charges anymore, the so–called Rayleigh limit is reached and fission into smaller droplets (Coulomb explosion) occurs. Two different models exist for the final formation of gas phase ions, the ion evaporation model (IEM) and the charge residue model (CRM). IEM assumes that instead of Coulomb explosion direct gas–phase ion emission from the droplet occurs when the droplet radius shrinks below 10 nm [6, 7]. CRM assumes that the gas phase ion develops from a very small droplet containing only one analyte ion which undergoes only evaporation of the remaining solvent [8]. IEM is experimentally well–supported for small organic and inorganic ions but for larger ions such as proteins the CRM seems to be more plausible [5].

Our ESI source is based on the design of the Aarhus group [9]. The heated stainless steel capillary counter electrode serves as an entrance for the electrosprayed ions into the vacuum system. Due to the electric potential and pressure difference across the capillary the ions enter into the first vacuum stage, where a roots pump (pump speed: 270 m^3/h) maintains a pressure of $\approx 5 \times 10^{-1}$ mbar. The capillary can be heated to evaporate remaining solvent molecules and to prevent cluster formation due to the temperature drop resulting from free expansion into the vacuum. The heating is realized with a Thermocoax heating wire wound around a segmented copper cylinder through which the capillary runs. The capillary has a length of 136 mm and an inner diameter of 0.51 mm. For e.g. the leu–enk experiments the capillary was heated up to 135° C. After leaving the capillary (bias typically +20 V), the ions

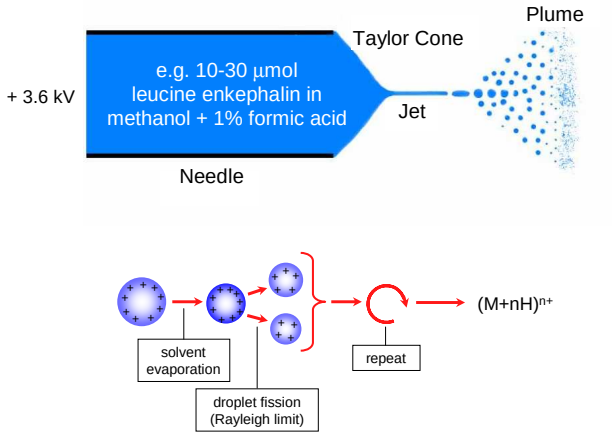

Figure 3.3: *Illustration of the ESI processes at atmospheric pressure. The positive ions due to the high voltage causes the formation of the Taylor cone and a jet, which splits into charged droplets (top). These droplets undergo solvation evaporation (bottom).*

traverse a distance of a couple of millimeters until they reach an aluminum skimmer of 1 mm diameter (bias typically +6 V) that separates first and second vacuum chamber and allows for differential pumping. The electric field between capillary and skimmer leads to acceleration of the ion in–between the successive collisions with residual gas. Declustering, de–solvation and collision induced dissociation can occur. The capillary is positioned slightly off–axis with respect to the skimmer orifice so that neutral background molecules are not directly sprayed through the skimmer orifice. The ions are focused back onto axis by a tube lens (typically + 250 V) through the skimmer into a second vacuum stage, where the pressure is kept at $\approx 3 \times 10^{-4}$ mbar by a turbo pump. The skimmer voltage can be pulsed up to 200 V to be able to block the ESI ions.

The ESI beam is too dilute to perform direct cross beam experiments and also the pressure in the second pumping stage is still too high for a good signal to noise ratio. Therefore the biomolecular ions are focused and guided by a radio frequency (RF) quadrupole ion guide and a mass filter into a lower–vacuum region. Then the ions are trapped in a RF trap, a so–called Paul trap, to achieve sufficient target density. In the following the operation of RF guiding, filtering and trapping will be explained.

3.4 RF guiding and trapping

In a periodic homogeneous electric field the time–dependent term of the force on a charged particle cancels out, but in a periodic quadrupole field a small average force drives charged particles back towards the center. The motion of a charged particle (with charge e and mass m) in a time–dependent electric field can be described with the equation

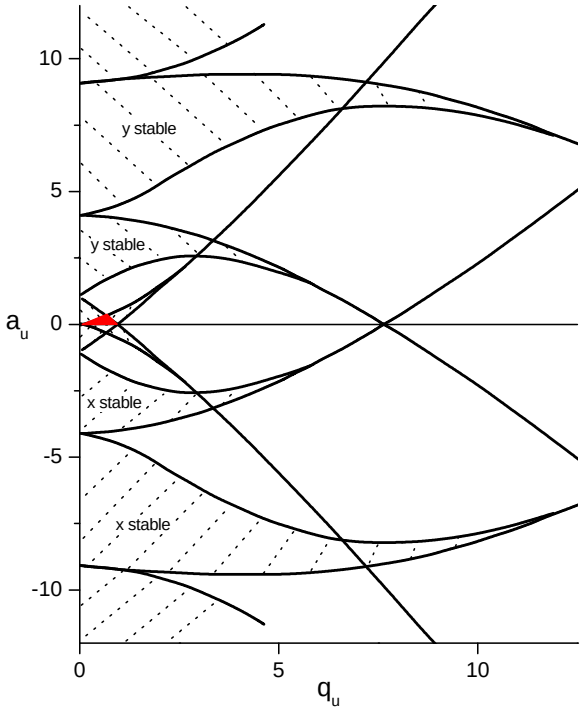

Figure 3.4: *Stability diagram for the two–dimensional quadrupole. A zoom into the red shaded triangle is shown in fig. 3.5.*

$$m\frac{d^2\vec{r}}{dt^2} = -e\nabla\Phi \tag{3.1}$$

The knowledge of the potentials $\Phi_{\pm} = \pm U \mp V\cos(\Omega t)$ on the (ideally hyperbolic) electrodes together with the Laplace condition allows to determine $\Phi(x,y)$ (for detailed derivation see [10] so that the equation of motion in one direction can be written as:

$$m\frac{d^2x}{dt^2} = \frac{-e}{r_0^2}(U + V\cos(\Omega t))x \tag{3.2}$$

where r_0 is a constant depending on the size of the quadrupole device.

In three dimensions, with the particle 3D coordinate u and dimensionless parameters ξ, a_u and q_u this can be written as:

$$m\frac{d^2u}{dt^2} = \frac{-m\Omega^2}{4}(a_u - 2q_u\cos(\Omega t))u \tag{3.3}$$

or

$$\frac{d^2u}{d\xi^2} + (a_u - 2q_u\cos(2\xi))u = 0 \tag{3.4}$$

This is the canonical form of the second–order linear differential Mathieu equation.
We obtain the parameters for 2–dimensional quadrupole ion guide and mass filter (with the x–y plane perpendicular to beam direction):

$$a_x = -a_y = \frac{4eU}{mr_0^2\Omega^2}; \qquad q_x = -q_y = \frac{-2eV}{mr_0^2\Omega^2} \tag{3.5}$$

For the 3–dimensional ion trap similar holds: $a_x = a_y = -2a_z$ and $q_x = q_y = -2q_z$.

The stability of an ion in these RF devices is only depending on the parameters a and q. Now we can map for example for a quadrupole ion guide the stability and instability regions in an a–q plot (see fig. 3.4). To guide the ion in the z–direction without hitting the rod electrodes, stable oscillations in x and y are required. The parameters a and q need to be located in the overlapping stability regions of x and y. Most devices operate in the stability region closest to the origin. Fig. 3.5 shows a zoom of the stability diagram into this region. Note, that for a fixed RF–frequency and a given mass, *a* depends solely on the DC voltage and *q* solely on the RF voltage. That means for a zero DC voltage the stability of an RF–only quadrupole is located on the x–axis with the broadest m/q transmission possible and this operation mode makes it suitable for an ion guide. When mass selection is required U and V are tuned for the selected mass in such a way that it lies close enough to the apex of the stability triangle to discriminate unwanted m/q values but at the same time maximize the transmission.

3.4.1 RF ion guide

The electrosprayed ions have to be transported through the region behind the skimmer, which is governed by a relatively high pressure of $\approx 10^{-3}$–10^{-4} mbar.

In the early days of ESI in the late 1980s, it was believed that the pressure in the ion guide should be as low as possible to prevent losses of ions by scattering with residual gas molecules. In an attempt to measure the *decrease* of ion transmission due to scattering losses at high pressures in an RF quadrupole ion guide of an ESI source Douglas and French observed an *increase* in ion transmission up to pressures of 1.1×10^{-2} mbar [11]. What is the reason for this increase?

As already mentioned earlier, ESI systems deal with low energetic ions originating from a high pressure region. According to Liouville's theorem, the phase space density of any system of particles subject to conservative forces behaves like an incompressible fluid. Focusing of an ion beam, i.e. an increase of position space density is thus only possible by a decrease of the momentum space density. A lower beam emittance could always be reached by substantial increase of the beam energy. But this is not an option here, since the ions need to be RF trapped eventually and kinetic energies have to be low. Alternatively, low beam emittance can be reached by introduction of dissipative forces to decrease the phase–space volume.

This is exactly what happens in a gas filled ion guide: Collisional damping of the ion trajectories confines the ions closer to the center [11]. The necessity of ion beam transport

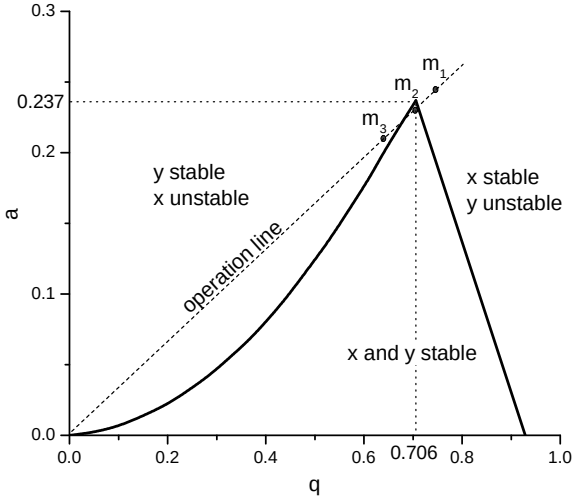

Figure 3.5: *Zoom of fig. 3.4 into the triangle closest to the origin. Mass m_2 is tuned into the apex and therefore mass–selected. Note that the a/q ratio is then also fixed for all other masses and thus all masses lie on the so–called operation line ($m_1 < m_2 < m_3$).*

through a high pressure region is thus an advantage because of collisional focusing effects when using an RF only ion guide.

For guiding purposes, the quadrupole geometry is of minor relevance with the exception that the length has to be sufficient to ensure collisional focusing. The quadrupole ion guide employed in the Paultje setup has a length of 117 mm and cylindrical rods with a diameter of 2 mm and an inscribed radius of 2.8 mm. Typical operation frequencies are 600–1500 kHz with a peak–to–peak voltage of 280 V.

For the RF–only voltage supply a home–built broadband balun was developed. The design allows tuning of the frequency between 500 kHz–10 MHz independent of the RF voltage. The frequency source used is based on the Direct Digital Synthesis (DDS) technique which allows very precise frequency tuning from a stable quartz–crystal oscillator frequency source. The output from the frequency generator was fed into a broadband power amplifier (ENI, model 3100L) to reach the required peak–to–peak voltage (50 W were required for 280 V peak–to–peak). The principle of the balun is shown in the circuit of fig. 3.6: The unbalanced to balanced back to unbalanced configuration of cascaded transformers makes the connection into a 50 Ω unbalanced termination load easy. The balanced part, connected to the quadrupole, is floating and can be lifted with a bias voltage. The balanced lines A and B are 180 degrees phase–shifted. A photograph of the actual balun can be found in fig. 3.7.

3.4.2 RF mass filter

The ESI process can give rise to different protonation or deprotonation states of the analyte ion. Furthermore, solvent ions, analyte solvent complexes and other species can be

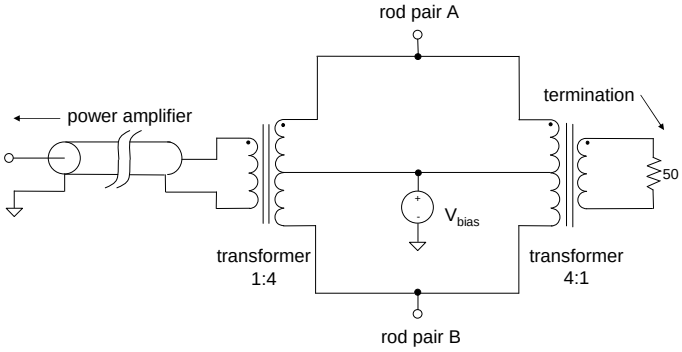

Figure 3.6: *Schematic circuit of the working principle of the balun.*

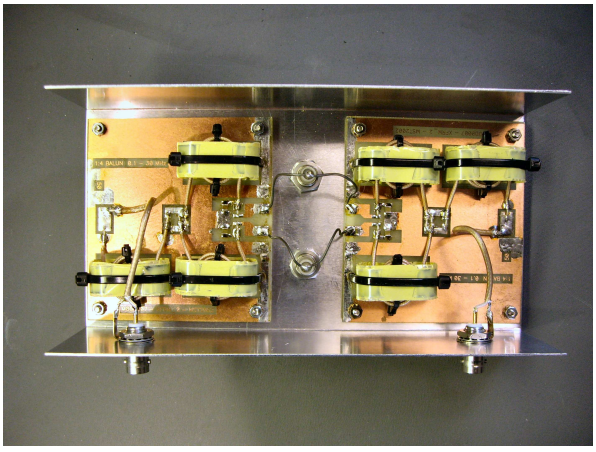

Figure 3.7: *Photograph of the balun.*

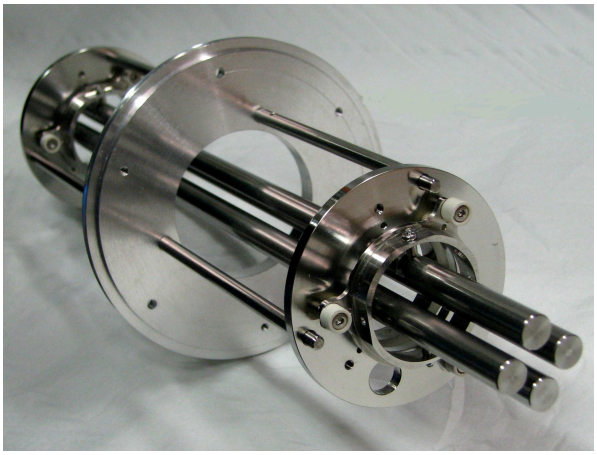

Figure 3.8: *Photograph of the mass filter.*

formed. These molecular ions partly undergo collision induced dissociation in the expansion region between the heated capillary and the skimmer. As a consequence, the m/q distribution of biomolecules passing the RF ion guide for a given analyte molecule usually contains many unwanted ions. To select only molecular ions with one particular m/q we designed a quadrupole mass filter ($a \neq 0$).

For m/q–filtering purposes, the quadrupole geometry is more important than for mere ion guiding, since operation takes place close to the apex of the stability region. A perfect quadrupole field can be generated by using hyperbolic electrodes. However, cylindrical rods are widely used because they are easier to manufacture and mount. For optimum approximation of the curvature of the hyperbolic electric field the diameter of the cylindrical rods should be [12]:

$$d = \frac{2r_0}{n-1} \tag{3.6}$$

with $2n$ being the number of circular rods of the RF–multipole and r_0 the inscribed radius. Dayton *et al.* [13] showed that for a quadrupole (n=2) the relation between rod diameter and inscribed radius should be:

$$d = 2r_0 \times 1.148 \tag{3.7}$$

Our home–built mass filter (see fig. 3.8) has the length of 308 mm and the rods with d=9 mm inscribe a circle with r_0=3.92 mm to satisfy equation 3.7. A commercial quadrupole power supply (QPS-105, Ardara) was chosen which can supply maximum RF peak–to–peak voltage of 2000 V and a DC voltage range of -200 V to +200 V. The power supply is based on a self–oscillating circuit which adjusts the output frequency for a wide range of capacitive loads. Attached to the quadrupole mass filter, the device has an RF frequency of $\approx$ 800 kHz.

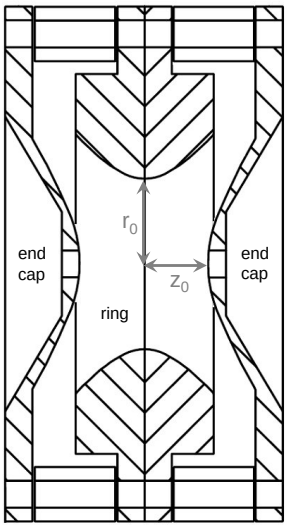

Figure 3.9: *Schematic cross–section of the ion trap. The size of the ring electrode is r_0=10 mm and the distance from the center to the end caps is z_0=7.07 mm.*

3.4.3 RF ion–trap

Behind the RF mass filter, the ions are focused by an Einzel lens into a 3D quadrupole ion trap. The stability triangle of the 3–dimensional ion trap looks very similar to the one of the 2–dimensional quadrupole in fig. 3.5. In the Paultje setup the RF–only mode is used for a broad mass range trapping. Ramping the RF and DC voltages in a given time could tune the masses sequentially into the apex and gives therefore the opportunity to take a mass spectrum, which is not possible using the relatively basic RF–only power supply currently attached to Paultje.

The ion trap was manufactured by Jordan TOF Products. A schematic cross–section of the trap, consisting of a hyperbolic ring electrode and two hyperbolic end cap electrodes, is shown in fig. 3.9. Fig. 3.10 shows a photograph of the trap mounted in the setup. For an ideal quadrupole field the relation $r_0^2 = 2z_0^2$ [10] determines the geometry of many commercial traps to r_0=10 mm for the ring electrode and z_0=7.07 mm for the distance from the center to the end caps. The size of the entrance and exit holes in the ring and end caps have diameters of 2.4 mm and 3 mm respectively. The RF–only power supply (D–1230, Jordan TOF Products) delivers a peak–to–peak voltage of 0–2500 V at 1 MHz to the trap ring electrode. Typical RF voltages for the experiments with leucine enkephalin were V_{pp}=1500 V and V_{pp}=2100 V. The base pressure inside the trap chamber is $\approx 1 \times 10^{-9}$ mbar.

For optimum ion transport from the ion guide into the trap, the ion guide is biased typically to 4 V. The ion guide not only damps out ion motion perpendicular to the axis, but also thermalizes the axial kinetic energy of the ions to $\approx$ 1–2 eV [11]. When the ions eventually reach the (grounded) entrance electrode of the RF–trap, consequently 5–6 eV of kinetic

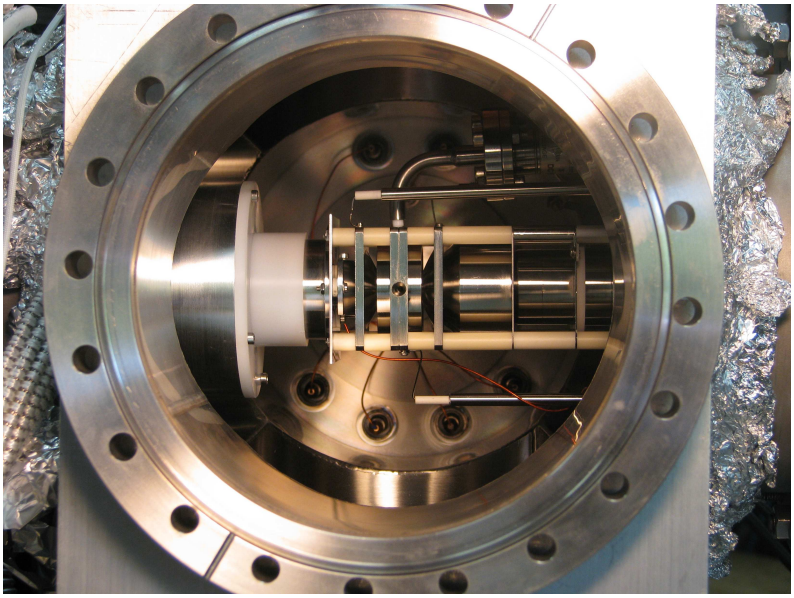

Figure 3.10: *Photograph of the ion trap (center) implemented into the set up. On the left side the cover of the mass filter can be seen, on the right side the focusing lenses and above these, a buffer gas valve is visible.*

energy has to be dissipated.

To this end, Helium buffer gas pulses up to a pressure of $\approx 10^{-3}$ mbar are introduced by a solenoid pulsed valve (Parker). The motions of the ions far from the center are damped by collisions with the buffer gas and focused to the center. Not only trapping efficiency is increased, but also extraction through the end cap hole is facilitated.

The trapped molecular ions are then exposed for up to several hundreds of ms to the ion or photon beam. The conditions were chosen such that a total of about 10% of the trapped protonated peptides were dissociated by collisions with the projectiles. Directly after the projectile beam pulse, a second He–buffer gas pulse can be applied to the trap, to cool energetic dissociation products (see fig. 3.11).

For ion extraction the RF voltage is switched off and an extraction voltage to the end caps is applied. The rising edge of a TTL signal triggers the RF shutoff in a crowbar fashion: The RF is set to zero after the next zero voltage crossover into positive direction. A delay of 0.5 μs after RF shutdown (adjustable from 200 ns before RF shut off to 4 μs after) is required to allow the ringing of the RF signal to decay. After that an extraction pulse of 3.5 μs duration biases the trap end caps to $U_{bias} = \pm$ 200 V.

When the extraction is completed, the RF of the ring electrode is switched on again. It needs about 100 μs to attain the initial amplitude.

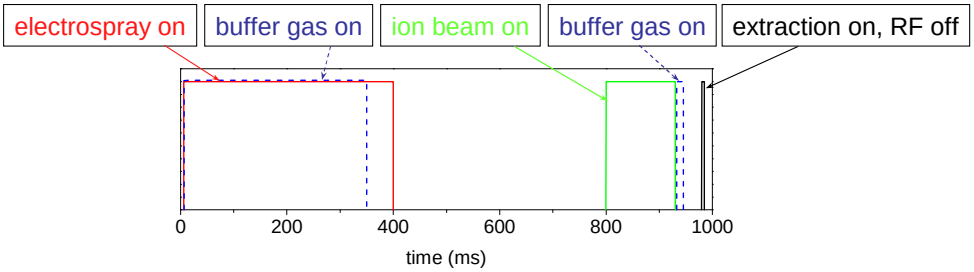

Figure 3.11: *A typical pulse scheme of the inclusive scan cycle. To obtain the different successive mass scans (see text) the electrospray or the projectile beam pulse can be blocked.*

3.5 Time–of–flight mass spectrometry and ion detection

The extraction pulse accelerates trapped protonated biomolecular ions and their cationic dissociation products into a linear time–of–flight (TOF) mass spectrometer (length flight tube: 82 cm, m/Δm = 200). The ions were detected by a silhouette–type micro–channel–plate detector (MCP, chevron configuration, diameter: 50 mm) with the front plate biased to -5 kV and the anode kept at ground potential (El–Mul). The detector signal was recorded by a 1–GHz digitizer (Ztec).

Despite the low background pressure and a liquid nitrogen cooled cryo–trap close to the RF–trap, contamination of the buffer gas or neutral molecules from the ESI source may contribute to the mass spectra. To extract the mass spectrum due to molecule fragmentation only, the data acquisition was divided into successive cycles of three mass scans. In each cycle, first the TOF spectrum resulting from irradiation of trapped molecules and neutral residual gas is recorded (inclusive scan, see fig. 3.12a). To obtain the net effect of irradiation upon the trapped protonated molecules, in a second scan the ECR source is switched off and a TOF spectrum of the initial trap content only was recorded (see fig. 3.12b). For the third scan, the ESI source was switched off and the TOF spectrum resulting from the ion–induced ionization of residual gas molecules was recorded (see fig. 3.12c). The latter two spectra are then subtracted from the inclusive scan. A typical pulse scheme of the scans is shown in fig. 3.11. A three–scan cycle took about 3–6 s. To obtain the final mass spectra a series of several thousand cycles is accumulated, which assures that long term fluctuations of molecule- and projectile–ion current are averaged out. The pulses were provided by a digital pulse/delay generator (model 565, Berkeley nucleonics) which was controlled by a home–built LabVIEW application. This application recorded at the same time also the data.

With a single particle signal height of $\approx$ 30 mV and 2 ns width the minimum number of trapped ions is estimated from the integral of the ESI peak to be $\approx$ 2000. Based on the assumption that 10% of the total number of MCP channels, i.e. $\approx 10^6$ channels, are hit all at once by 2000 ions, implies 2×10^6 channels of the second plate to be bleached [14]. This indicates that the detector operates in the non–linear saturation regime. The number 2000 is thus a strong underestimation of the real number of ions being trapped.

Two lenses behind the ion trap (see fig. 3.1) focus the extracted ion beam onto the detector

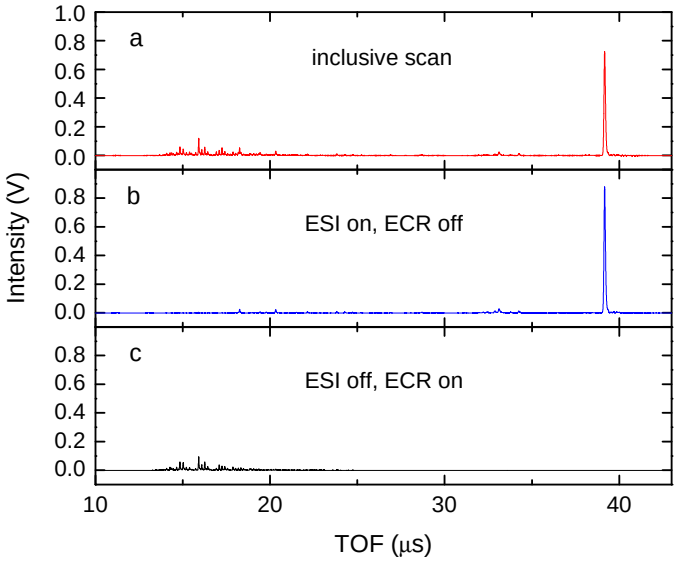

Figure 3.12: *The successive cycles of three mass scans (see text).*

and therefore influence the time resolution of the TOF spectrometer (see fig. 3.13). Note, that no Wiley McLaren TOF design is used, where double focusing is applied to compensate for temporal, spatial and initial kinetic energy distributions [15]. Different voltage settings vary also the spot size of the ion beam onto the detector. The different beam spot size changes the level of detector saturation and makes finding the perfect settings a bit more difficult.

3.6 ECRIS

The ion–induced fragmentation studies were performed with an ion beam extracted from an Electron Cyclotron Resonance Ion Source (ECRIS) installed at the ZernikeLEIF facility of the Kernfysisch Versneller Instituut (KVI) in Groningen. A magnetic bottle is superimposed from a longitudinal magnetic field generated by two coils and from a radial field supplied by a permanent hexapole magnet. Within this magnetic bottle electrons gyrate due to the Lorentz force with the cyclotron frequency $\omega_c = 2\pi eB/m_e$ [16]. Applying now low gas pressure of the desired ion species and a 14 GHz–RF field with the same frequency as ω_c a plasma arises where the electrons are resonantly accelerated. The electrons can gain high energies and ionize atoms and ions by (multiple) collisions. High charge states can be achieved (up to Xe^{25+}) [17]. The source is operated with high voltages from 2–25 kV. The ions are extracted by an extraction lens, mass–to–charge ratio selected by a 110° analyzing magnet and guided to the experimental setup by a series of quadrupole magnets and a 45° deflection magnet.

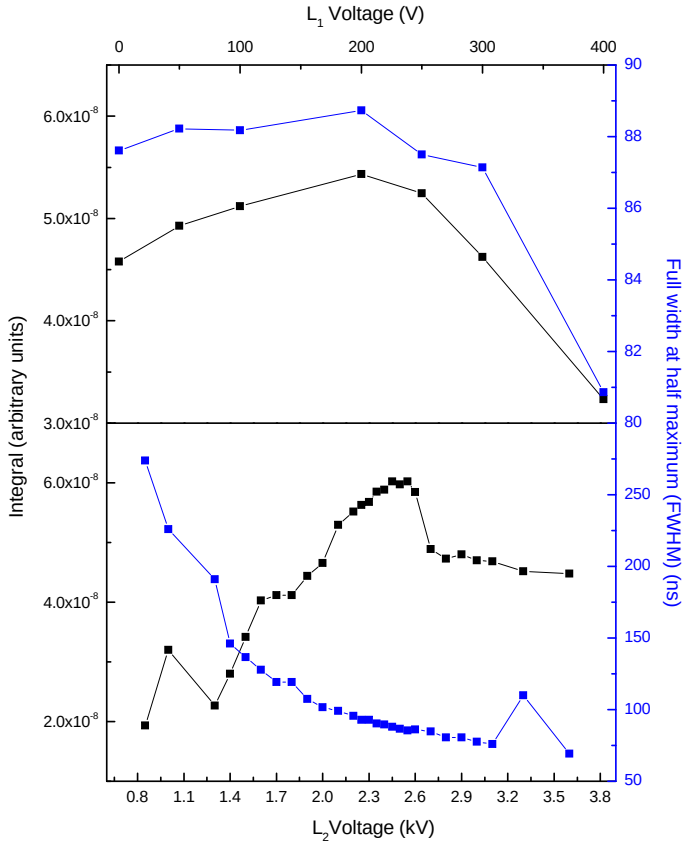

Figure 3.13: *Influence of the focusing lenses L_1 and L_2 voltages on the width and integral of the leucine enkephalin peak.*

3.7 BESSY II

The photon–induced fragmentation studies presented in chapter 7 were conducted with the quasi–periodic undulator U125/2 [18] of the 3rd generation synchrotron facility Berliner Elektronenspeicherring Gesellschaft für Synchrotronstrahlung (BESSY II) in Berlin. A synchrotron is a cyclic particle accelerator in which the magnetic field and the electric field are synchronized with the traveling particle beam to circulate and accelerate the particles. At BESSY electrons can be accelerated to an energy of up to 1.7 GeV and are subsequently injected into a storage ring. There exist 11 different permanent magnet undulators to provide different photon energy ranges to the user experiments.

An undulator consists of a periodic structure of alternating dipole magnets. The static alternating magnetic field lets the traversing electrons oscillate and radiate.

The undulator U125/2 consists of dipole magnets with 32 periods each 125 mm long

and provides high brilliance and flux in the energy range of 20-500 eV. The gap between the magnets determines the oscillation frequency. Minimum gap here is 15.7 mm. To prevent transmission of higher harmonics through the monochromator and contamination of the experimental data the undulator has dislocations in the periodic pattern and is thus quasi–periodic.

Tunable VUV photons in the energy range of 8–40 eV were obtained with the 10 m focal length normal incidence monochromator (NIM) [19]. The monochromator is an off–Rowland circle normal incidence monochromator [20] consisting of an entrance and exit slit and a spherical grating with a 10 m focus and 2° vertical deflection. In order to achieve maximum photon flux a relatively low–resolution gold–coated 300 l/mm grating was employed. The slits are rotatable by $\pm\ 2^\circ$ and the slits widths can be varied from 0–2000 μm. A horizontally deflecting toroidal mirror and a vertically demagnifying plane ellipse mirror focus the beam on the entrance slit. Two toroidal mirrors focus the beam into the experimental setup.

References

[1] O. Hadjar, *Hidden sides of C_{60}*, PhD thesis, Kernfysisch Versneller Instituut, University of Groningen, 2001.

[2] F. Alvarado, *Ion induced radiation damage on the molecular level*, PhD thesis, Kernfysisch Versneller Instituut, University of Groningen, 2007.

[3] J. Fenn, Angew. Chem.-Int. Edit. **42**, 3871 (2003).

[4] A. Bruins, J. Chromatogr. A **794**, 345 (1998).

[5] P. Kebarle and U. H. Verkerk, Mass Spectrom. Rev. **28**, 898 (2009).

[6] J. Iribarne and B. Thomson, J. Chem. Phys. **64**, 2287 (1976).

[7] B. Thomson and J. Iribarne, J. Chem. Phys. **71**, 4451 (1979).

[8] M. Dole, L. Mack, and R. Hines, J. Chem. Phys. **49**, 2240 (1968).

[9] T. Jørgensen, J. Andersen, P. Hvelplund, and M. Sørensen, Int. J. Mass Spectrom. **207**, 31 (2001).

[10] R. March, J. Mass Spectrom. **32**, 351 (1997).

[11] D. Douglas and J. French, J. Am. Soc. Mass Spectrom. **3**, 398 (1992).

[12] D. Gerlich, Adv. Chem. Phys. **82**, 1 (1992).

[13] I. Dayton, F. Shoemaker, and R. Mozley, Rev. Sci. Instrum. **25**, 485 (1954).

[14] D. Anacker and J. Erskine, Rev. Sci. Instrum. **62**, 1246 (1991).

[15] W. Wiley and I. Mclaren, Rev. Sci. Instrum. **26**, 1150 (1955).

[16] A. Drentje, Rev. Sci. Instrum. **74**, 2631 (2003).

[17] F. W. Meyer and M. I. Kirkpatrik, editors, *Proceedings of the 10th International Workshop on ECR Ion Sources*, Oak Ridge, 1990, Rep. No. Conf.-9011136.

[18] J. Bahrdt, W. Frentrup, A. Gaupp, M. Scheer, W. Gudat, G. Ingold, and S. Sasaki, Nucl. Instrum. Meth. A **467**, 130 (2001).

[19] G. Reichardt, J. Bahrdt, J. Schmidt, W. Gudat, A. Ehresmann, R. Muller-Albrecht, H. Molter, H. Schmoranzer, M. Martins, N. Schwentner, and S. Sasaki, Nucl. Instrum. Meth. A **467**, 462 (2001).

[20] J. Samson, *Techniques of Vacuum Ultra Violet Spectroscopy*, Wiley, 1967.